

Terahertz gain on shallow donor transitions in silicon

R. Kh. Zhukavin^{a)} and V. N. Shastin

Institute for Physics of Microstructures, Russian Academy of Sciences, 603950 Nizhny Novgorod, Russia

S. G. Pavlov and H.-W. Hübers

Institute of Planetary Research, German Aerospace Center (DLR), 12489 Berlin, Germany

J. N. Hovenier and T. O. Klaassen

Kavli Institute of Nanoscience Delft, Delft University of Technology, 2600 GA Delft, The Netherlands

A. F. G. van der Meer

FOM-Institute for Plasma Physics, 3439 MN Nieuwegein, The Netherlands

(Received 27 July 2007; accepted 13 September 2007; published online 7 November 2007)

Small signal gain measurements of optically excited terahertz silicon lasers are reported. Two types of lasers, Si:P and Si:Bi, were investigated. They were optically excited with radiation from a free electron laser or a CO₂ laser. The experiments were performed with an oscillator-amplifier scheme where one sample serves as a laser while the other one is an amplifier. In case of the free electron laser the pump frequency corresponds to intracenter excitation of the $2p_0$ or $2p_{\pm}$ states of the P and Bi Coulomb centers, and the gain was determined for the $2p_0 \rightarrow 1s(E)$, $2p_0 \rightarrow 1s(T_2)$ transitions in Si:P and the $2p_{\pm} \rightarrow 1s(E)$ transition in Si:Bi. Pumping with a CO₂ laser leads to photoexcitation of the Coulomb centers. In this case the gain was determined for the $2p_0 \rightarrow 1s(T_2)$ of Si:P transition. The gain for intracenter pumping is in the range 5–10 cm⁻¹ while for photoexcitation the gain is considerably less, namely ~ 0.5 cm⁻¹. The experimental results are analyzed and found to be in good agreement with theoretical calculations based on balance equations. © 2007 American Institute of Physics. [DOI: 10.1063/1.2804756]

I. INTRODUCTION

Nowadays various semiconductor devices are used for the generation of terahertz (THz) radiation.¹ Significant achievements have been obtained with III–V heterostructures. However, oscillators based on silicon have several potential advantages compared with GaAs quantum cascade lasers. Two major advantages are low lattice absorption and the possibility of monolithic integration with silicon microelectronics.² Many efforts have been made to transfer the principles of quantum cascade schemes from GaAs-based^{3,4} to Si/SiGe or SiGe/Ge structures.^{5,6} Nevertheless, up to now THz lasing has been obtained only in bulk silicon doped by shallow donors, which are optically excited.^{7–12} There are two basic mechanisms that can cause population inversion of optically excited electrons between donor states in bulk silicon at temperatures below 30 K. The first one is observed in Si:P, where the lifetime of the upper laser level, $2p_0$, is controlled by the interaction with intervalley g -LA and f -TA phonons while decay of electrons from the lower laser levels, $1s(E)$ and $1s(T_2)$, occurs through the emission of intervalley g -TA phonons. The lifetimes are approximately 50–60 ps for the $2p_0$ (Ref. 13) and ~ 10 ps for the $1s$ states,¹⁴ respectively. In Si:P, direct pumping into the $2p_0$ state results in stimulated emission at 58.49 μm [$2p_0 \rightarrow 1s(E)$ transition] while pumping in the higher donor states as well as in the conduction band yields emission at 55.33 μm [$2p_0 \rightarrow 1s(T_2)$ transition]⁹ (Fig. 1). Another

mechanism for population inversion was observed in Si:Bi. It is due to a strong coupling of the $2p_0$ and $2s$ states with the $1s(A_1)$ ground state via intervalley f -TO, g -LO phonons. In Si:Bi the spontaneous emission of optical phonons makes the lifetimes of the $2p_0$ and $2s$ states extremely short,¹⁵ dumping carriers directly to the ground state. Such a scenario provides the depletion of the $2p_0$ and $2s$ states and leads to a negligible population of the $1s(E)$ and $1s(T_2)$ states. Hence, population inversion between the $2p_{\pm}$ (lifetime ~ 40 – 50 ps)¹⁶ and the $1s(E)$, $1s(T_2)$ states is created. Intracenter pumping of the $2p_{\pm}$ state results in lasing on the $2p_{\pm} \rightarrow 1s(E)$ transition at 52.32 μm , while the pumping of the $2p_0$ state leads to the lasing on the $2p_0 \rightarrow 1s(E)$ [64.52 μm (Ref. 10)]. Previously performed experiments revealed that intracenter resonant pumping leads to much lower thresholds in comparison with CO₂ laser pumping.¹¹ Here we report on small signal gain measurements in Si:P and Si:Bi under intracenter pumping of the $2p_0$ and $2p_{\pm}$ states with radiation from the free electron laser FELIX. Gain measurements of Si:P under pumping with a CO₂ laser are also presented.

II. EXPERIMENTAL SETUP

The gain measurements were performed using an oscillator-amplifier scheme, where one sample acts as the laser and the other one amplifies the laser radiation, which is transmitted through the second sample (Fig. 2). The Si:P samples were prepared from float zone grown Si:B crystals. By neutron transmutation a phosphorus concentration of $N_D = 3 \times 10^{15}$ cm⁻³ with a compensation of $N_A/N_D \approx 0.35$ (N_A : acceptor concentration) was realized. The Si:Bi samples

^{a)}Author to whom correspondence should be addressed. Electronic mail: zhur@ipm.sci-nnov.ru

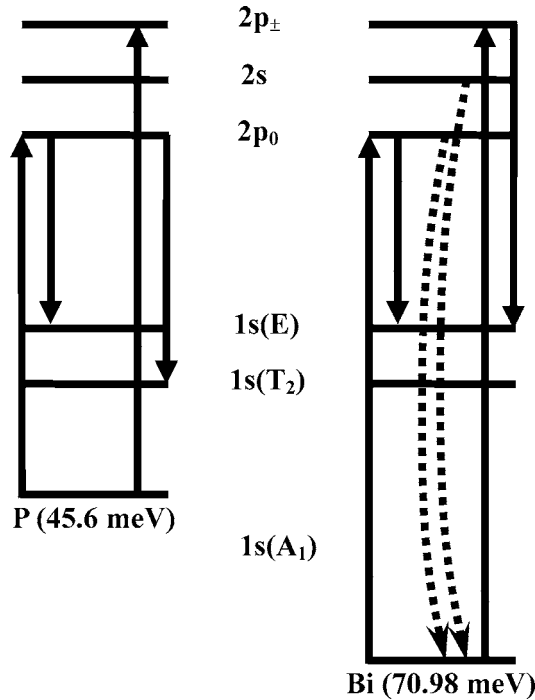


FIG. 1. Principal states involved in population inversion in Si:P (left) and Si:Bi (right) (not to scale). The arrows up indicate pump transitions. The arrows down indicate the laser transitions. For Si:Bi the optical phonons, which deplete the $2p_0$ and $2s$ states, are shown by dotted arrows.

were grown by the float zone technique with concentration $\sim 10^{16} \text{ cm}^{-3}$ and doping was done during the crystal growth. The laser was cut in the form of a $7 \times 5 \times 1.5 \text{ mm}^3$ rectangular parallelepiped. Its facets were optically polished with each pair of opposite facets parallel with an accuracy of 1 arc min. This yields a high quality laser resonator based on internal reflections modes. The shape of the amplifier sample was prepared in an irregular way in order to avoid lasing. The dimensions were $(6-7) \times 5 \times (1-1.5) \text{ mm}^3$ (Fig. 2). The pump radiation from the free electron laser was delivered to the $7 \times 5 \text{ mm}^2$ and $5 \times (6-7) \text{ mm}^2$ facets of the la-

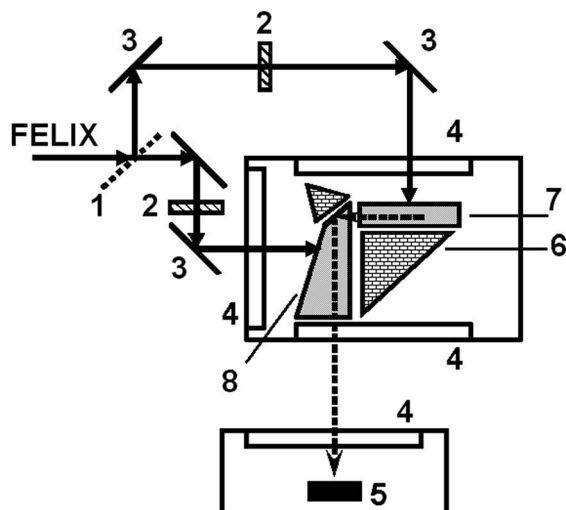


FIG. 2. Sketch of the experimental setup for pumping with the free electron laser FELIX: (1) beam splitter, (2) attenuators, (3) mirrors, (4) optical windows, (5) Ge:Ga detector, (6) metal screen, (7) laser, (8) amplifier.

ser and the amplifier, respectively. The samples were cooled to about 6 K in a liquid helium (LHe) flow cryostat. The THz emission left the flow cryostat transversely to the pump radiation. In addition, z -cut quartz was used as an output window and filter in order to block any leakage of pump radiation. The output emission from the Si:P or Si:Bi crystals was registered by a LHe cooled Ge:Ga photodetector with a maximum sensitivity in the wavelength range of $50 - 120 \mu\text{m}$ and with a response time of $\sim 3 \text{ ns}$.

The free electron laser FELIX was used as the pump source and was tuned in the wavelength range from 17 to $37 \mu\text{m}$. Its emission consists of $6 \mu\text{s}$ long macropulses with a repetition rate of 5 Hz . Each macropulse consists of a train of $\sim 5 \text{ ps}$ short micropulses separated by 1 ns time intervals. In a special operation mode the micropulse separation is 20 ns . The maximum macropulse energy was $\sim 15 \text{ mJ}$ (1 ns micropulse separation). This corresponds to an average power of $\sim 2.5 \text{ kW/cm}^2$ during a macropulse, or $\sim 0.5 \text{ MW/cm}^2$ for the micropulse. The radiation from FELIX was divided into two parts by a Mylar beam splitter. One part was used as a pump for the laser (L -beam). It contained 20% of the total output power, which was much higher than the laser threshold. The second one (A -beam) was delivered to the amplifier. The power of the second part was controlled by variable absorbers. The macropulse energy of both parts was measured with a joule meter. The power incident on the laser and the amplifier was recalculated taking into account reflection from windows in the cryostat. Approximately half of the output power from FELIX reached the samples. Both beams could be either completely closed or attenuated. The signal measured with open L -beam and closed A -beam is the pure laser signal, corresponding to the initial laser intensity. The signal with both L -beam and A -beam open represented the amplified intensity. No signal was detected with closed L -beam and opened A -beam (spontaneous emission of amplifier) as well as with both beams closed.

For the investigation of the gain in Si:P under photoionization by radiation of CO_2 laser ($10.6 \mu\text{m}$ or 117 meV , maximum intensity 500 kW/cm^2) a similar setup was used. The scheme is shown in Fig. 3. Instead of a flow cryostat the Si laser was immersed in LHe by use of a dipstick. The laser sample was prepared in the shape of a rectangular parallelepiped (with dimensions of $7 \times 7 \times 5 \text{ mm}^3$) with polished facets. The amplifier sample had the same dimensions with worse polishing of the facets in order to suppress lasing. The doping levels were $3 \times 10^{15} \text{ cm}^{-3}$ and $2 \times 10^{15} \text{ cm}^{-3}$ for the laser and amplifier, respectively. The CO_2 laser beam was divided into two parts in order to irradiate the $7 \times 7 \text{ mm}^2$ facets of both samples. A photon drag monitor served for CO_2 laser power measurements.

III. ANALYSIS PROCEDURE

From the shape of the emission pulses measured with a 20 ns micropulse separation of FELIX and of the Si laser (Fig. 4) we can determine the resonator loss and conclude that the lifetime of a photon in the laser resonator, τ_{res} , is about 10 ns .¹⁷ For the analysis we assume that for both la-

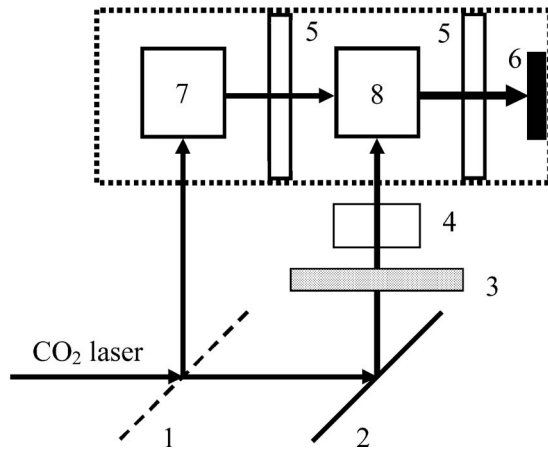


FIG. 3. Sketch of the experimental setup for gain measurements with CO₂ laser pumping: (1) beam splitter, (2) mirror, (3) attenuator, (4) photon drag monitor, (5) sapphire filters, (6) Ge:Ga detector, (7) Si:P laser, (8) Si:P amplifier.

ers, Si:P as well as Si:Bi, and for all emission frequencies, the photon lifetime in the cavity of the laser samples is $\tau_{\text{res}} = 10$ ns, which corresponds to a resonator loss of $\gamma = 0.01 \text{ cm}^{-1}$. Thus with respect to the laser emission with a 1 GHz repetition rate we can neglect the micropulse structure and consider the output emission to be continuous during the macropulse duration. If the lifetime of population inversion, τ , is longer than ln/c (l is the amplifier length, n is the refractive index of Si, and c is the speed of light), we can assume that the THz radiation passing the active medium will be amplified during the whole transit time, otherwise the time of amplification is equal to the lifetime of the upper laser state, which is, in fact, close to the population inversion lifetime. Hence, for pulsed population inversion and $\tau \geq ln/c$ the intensity of the radiation I_1 at the output of the amplifier with length l can be written as

$$I_1 = I_0 \left(\frac{\tau}{T_F} e^{\alpha_p l} + \frac{T_F - \tau}{T_F} \right). \quad (1)$$

Here I_0 is the intensity of the radiation, which enters the amplifier, α_p is the pulsed gain, and T_F is the micropulse

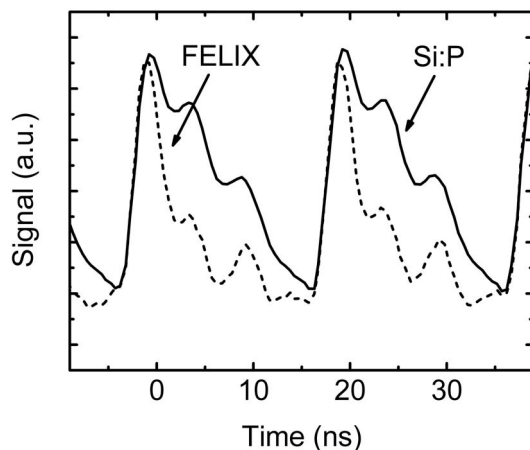


FIG. 4. Emission pulses of the Si:P laser and the free electron laser FELIX (normalized to the peak of the Si:P emission). The pulse period is 20 ns. The pump frequency corresponds to the $1s(A_1) \rightarrow 2p_0$ transition.

period. As can be seen, amplification occurs during the lifetime of population inversion. The rest of the time ($\tau \leq T_F$) the radiation passes the amplifier without change. Here it is assumed that the losses (e.g., due to lattice absorption or D^- center absorption) are equal for the open and closed A-beam. The pulsed gain α_p , which exists during the lifetime of the population inversion, can be written as

$$\alpha_p = \frac{1}{l} \ln \left(\left(\frac{I_1}{I_0} - 1 \right) \frac{T_F}{\tau} + 1 \right). \quad (2)$$

Note that in the case of direct pumping into the $2p_0$ state the amplification continues during the lifetime of the $2p_0$ state while pumping of the $2p_{\pm}$ state prolongs the amplification process. In Si:P it lasts throughout the consecutive relaxation of the $2p_{\pm}$, $2s$, and $2p_0$ states. In the case of $\tau < ln/c$, Eqs. (1) and (2) have to be modified by replacing l with $c\tau/n$.

In the case of pumping with a CO₂ laser the duration of the Si:P emission is ~ 50 ns. Thus, for the interpretation of the experimental data a multireflection approach, which takes into account partial reflection of the Si laser radiation at the facets of the amplifier, was used. Under such conditions the following equation presents the relationship between I_1 , I_0 , l , and α :

$$\frac{I_1}{I_0} \sum_{N=0}^{\infty} R^{2N} = \sum_{N=0}^{\infty} R^{2N} e^{(2N+1)\alpha l}, \quad (3)$$

where $N=0, 1, 2, \dots$, and $R=(n-1)^2/(n+1)^2$.

IV. EXPERIMENTAL RESULTS AND DISCUSSION

Figure 5 displays the pulsed gain as a function of pump energy and pumping rate. The gain was determined according to Eq. (2). The highest pulsed gain of $\sim 5.3 \text{ cm}^{-1}$ at 1.2 mJ ($\sim 0.04 \text{ MW/cm}^2$ per micropulse) was obtained for Si:P under resonant pumping into the $2p_0$ state [Fig. 5(a)]. For pumping into the $2p_{\pm}$ state the maximum observed gain was $\sim 6 \text{ cm}^{-1}$ at 5–6 mJ (~ 0.18 – 0.2 MW/cm^2 per micropulse) [Fig. 5(b)]. Nevertheless, the parameter “gain per unit power” was less than for pumping into the $2p_0$ state. The latter is in qualitative agreement with previously obtained data on the laser threshold for Si:P lasers under resonant pumping: namely, the threshold for laser emission from the $2p_0 \rightarrow 1s(E)$ transition is always less than for the $2p_0 \rightarrow 1s(T_2)$ transition.¹¹ Despite a greater cross section and more efficient pumping for the $1s(A_1) \rightarrow 2p_{\pm}$ transition compared with the $1s(A_1) \rightarrow 2p_0$ transition¹⁸ the pulsed gain per unit power is larger for laser emission originating from the $2p_0$ state. Figure 5(c) shows the result of the measurements for Si:Bi under resonant pumping of the $2p_{\pm}$ state. This leads to stimulated emission on the $2p_{\pm} \rightarrow 1s(E)$ transition. The maximum gain was measured to be ~ 9 – 10 cm^{-1} at 3–6 mJ (~ 0.1 – 0.2 MW/cm^2 per micropulse). No amplification was measured at a pump frequency corresponding to the $1s(A_1) \rightarrow 2p_0$ transition. The latter can be explained by the small gain on the $2p_0 \rightarrow 1s(E)$ transition. That is because of strong coupling of the $2p_0$ state with the f -TO optical phonon, which results in a short lifetime of this state. This is supported by the fact that the laser threshold for excitation into $2p_0$ is the highest one.¹¹ The smaller gain per unit power and

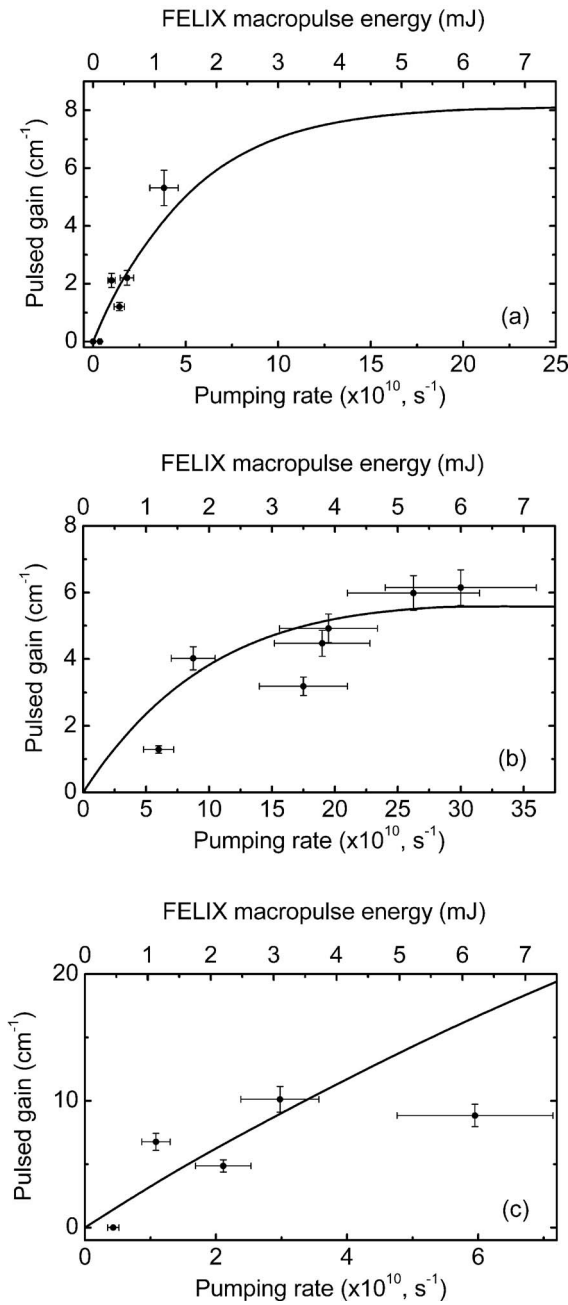


FIG. 5. Pulsed gain of the (a) $2p_0 \rightarrow 1s(E)$ and (b) $2p_0 \rightarrow 1s(T_2)$ transitions of the Si:P laser and of the $2p_{\pm} \rightarrow 1s(E)$ transition of the Si:Bi laser as a function of the FELIX macropulse energy (dots: experimental data; straight lines: model calculation based on the solution of balance equations).

concentration for Si:Bi in comparison with Si:P can be explained by a smaller peak cross section of the laser transition caused by concentration broadening, which becomes significant for concentrations of 10^{16} cm^{-3} (Ref. 18).

The measured gain can be compared with calculations (Fig. 5, solid lines). These are based on the solution of balance equations. The pulsed gain for Si:P and Si:Bi was calculated taking into account the population of the $1s(A_1)$, $1s(E)$, $1s(T_2)$, $2p_0$, $2s$, and $2p_{\pm}$ states and the conduction band population under optical pumping of a particular state. For the pump pulse it was assumed that it has a Gaussian shape with a full width at half maximum of 10 ps. This is longer than the actual length of the pulse delivered by

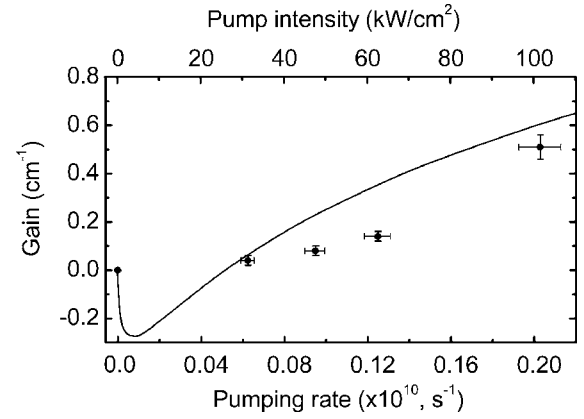


FIG. 6. Gain of the transitions $2p_0 \rightarrow 1s(T_2)$ in Si:P when excited with a CO_2 laser (dots: experimental data; straight line: model calculation based on the solution of balance equations).

FELIX due to reflections in the amplifier sample. The optical cross sections needed for the calculations were taken from the literature.¹⁹ As can be seen for Si:P the agreement between measurement and calculation is quite good. On the contrary for Si:Bi we can note a deviation between theoretical curve and experimental data. It is possible to explain this deviation in the frame of the model used for calculation. The cross sections taken from Refs. 15 and 19 correspond to a smaller concentration of donors ($2 \times 10^{15} \text{ cm}^{-3}$). In our case line broadening can be expected. First, that leads to the better overlapping of the absorption line and FELIX spectrum and results in an increase of pumping rate. Second, the line broadening decreases the peak value of the cross section for the $2p_{\pm} \rightarrow 1s(E)$ transition.

As follows from the above description of the experiment the measured value is an “instant” gain with a decay time equal to the lifetime of the upper laser level or the sum of lifetimes of excited states. On one hand, the use of short pulse excitation allows us to determine cavity losses, which are so small that they can be neglected. On the other hand, for practical purposes the stationary gain α_s is needed. Generally we can use the gain averaged over the macropulse duration:

$$\alpha_s \approx \frac{\alpha_p}{(T_F/\tau_F)(v_p\tau_F)} - \gamma = \frac{\alpha_p}{T_F v_p} - \gamma, \quad v_p < 1/\tau_F, \quad (4)$$

where v_p is the pumping rate for pulsed excitation, and τ_F is the micropulse duration. Here the ratio T_F/τ_F serves as an averaging factor. The presence of the product $v_p\tau_F$ is explained by the fact that for $v_p < 1/\tau_F$ we should take into account a lesser absorption of pump photons than for $v_p > 1/\tau_F$. For instance, for the $2p_0$ state in Si:P and an average pump intensity of 200 W/cm^2 , $\alpha=4 \text{ cm}^{-1}$ and $v_p=4 \times 10^{10} \text{ s}^{-1}$ [see Fig. 3(a)]; α_s can be estimated as 0.09 cm^{-1} .

Figure 6 shows the gain for photoexcitation with a CO_2 laser. It was obtained with use of Eq. (3) (dots). The measured gain values are in the range $0.1\text{--}0.5 \text{ cm}^{-1}$ for pump intensities of $30\text{--}100 \text{ kW/cm}^2$. In comparison with α_s for intracenter excitation there is a large difference in the pump intensity needed to obtain the same gain. This is explained mainly by two reasons: first, the ionization cross section for

a pump photon with an energy of 117 meV (about 4×10^{-16} cm²) is much smaller than the one for intracenter excitation ($\sim 10^{-14}$ cm²), and second, the presence of D⁻ centers (negatively charged donors), which have a rather large absorption at THz frequencies.²⁰ Also stronger heating of the Si sample by CO₂ laser radiation may reduce the gain. The result of the gain calculation is presented as well in Fig. 6. For the lifetimes the same parameters as for intracenter excitation were chosen. The parameters concerning the D⁻ centers were taken from Ref. 21. The negative gain at pump intensities below 20 kW/cm² is caused by the presence of the negatively charged donors. The overall agreement between calculations and experimental results is good.

V. SUMMARY

In summary, the small signal gain of optically excited Si:P and Si:Bi lasers has been determined by a laser-amplifier scheme. For intracenter excitation of Si:P the maximum gain is ~ 5.3 cm⁻¹ for the $2p_0 \rightarrow 1s(E)$ transition and ~ 6 cm⁻¹ for the $2p_0 \rightarrow 1s(T_2)$ transition. The intracenter excitation of Si:Bi gives a value 10 cm⁻¹ for the $2p_{\pm} \rightarrow 1s(E)$ transition while the gain at the $2p_0 \rightarrow 1s(E)$ transition was below the detection level of the experiment. Excitation of Si:P by CO₂ laser radiation yields a much smaller gain [~ 0.5 cm⁻¹, $2p_0 \rightarrow 1s(T_2)$]. This can be explained by the lower efficiency of the donor excitation process due to photoionization and D⁻ center absorption stronger heating of the Si sample. The obtained experimental data agree with theoretical calculations based on balance equations.

ACKNOWLEDGMENTS

We gratefully acknowledge the support by the Stichting voor Fundamenteel Onderzoek der Materie (FOM) in providing the required beam time on FELIX and highly appreciate the skilful assistance by the FELIX staff. This work was supported by the Deutsche Forschungsgemeinschaft (DFG) and the Russian Foundation for Basic Research (RFBR), RFBR Grant Nos. 05-02-16790 and 05-02-16734.

¹*Long-Wavelength Infrared Semiconductor Lasers*, Wiley Series in Lasers and Applications, edited by H. K. Choi (Wiley-Interscience, Hoboken, NJ, 2004), pp. 1–386.

- ²*Towards the First Silicon Laser*, NATO Science Series, edited by L. Pavesi, S. Gaponenko, and L. Dal Negro (Kluwer Academic, Dordrecht, 2003), Vol. 93, pp. 1–467.
- ³S. Kumar, B. S. Williams, Q. Hu, and J. L. Reno, *Appl. Phys. Lett.* **88**, 121123 (2006).
- ⁴R. Köhler, A. Tredicucci, C. Mauro, F. Beltram, H. E. Beere, E. H. Linfield, A. G. Davies, and D. A. Ritchie, *Appl. Phys. Lett.* **84**, 1266 (2004).
- ⁵K. Driscoll and R. Paiella, *Appl. Phys. Lett.* **89**, 191110 (2006).
- ⁶S. A. Lynch, R. Bates, D. J. Paul, D. J. Norris, A. G. Cullis, Z. Ikonic, R. W. Kelsall, P. Harrison, D. D. Arnone, and C. R. Pidgeon, *Appl. Phys. Lett.* **81**, 1543 (2002).
- ⁷S. G. Pavlov, R. Kh. Zhukavin, E. E. Orlova, V. N. Shastin, A. V. Kirsanov, H.-W. Hübers, K. Auen, and H. Riemann, *Phys. Rev. Lett.* **84**, 5220 (2000).
- ⁸S. G. Pavlov, H.-W. Hübers, M. H. Rummeli, R. Kh. Zhukavin, E. E. Orlova, V. N. Shastin, and H. Riemann, *Appl. Phys. Lett.* **80**, 4717 (2002).
- ⁹R. Kh. Zhukavin, D. M. Gaponova, A. V. Muravjov, E. E. Orlova, V. N. Shastin, S. G. Pavlov, H.-W. Hübers, J. N. Hovenier, T. O. Klaassen, H. Riemann, and A. F. G. van der Meer, *Appl. Phys. B: Lasers Opt.* **76**, 613 (2003).
- ¹⁰H.-W. Hübers, S. G. Pavlov, and V. N. Shastin, *Semicond. Sci. Technol.* **20**, S211 (2005).
- ¹¹V. N. Shastin, R. Kh. Zhukavin, E. E. Orlova, S. G. Pavlov, M. H. Rummeli, H.-W. Hübers, J. N. Hovenier, T. O. Klaassen, H. Riemann, I. V. Bradley, and A. F. G. van der Meer, *Appl. Phys. Lett.* **80**, 3512 (2002).
- ¹²S. G. Pavlov, H.-W. Hübers, J. N. Hovenier, T. O. Klaassen, D. A. Carder, P. J. Phillips, B. Redlich, H. Riemann, R. Kh. Zhukavin, and V. N. Shastin, *Phys. Rev. Lett.* **96**, 037404 (2006).
- ¹³V. N. Shastin, S. G. Pavlov, P. J. Phillips, D. A. Carder, T. O. Klaassen, J. N. Hovenier, H.-W. Hübers, R. Kh. Zhukavin, H. Riemann, B. Redlich, and A.F.G. van der Meer (unpublished).
- ¹⁴E. E. Orlova, *Proceedings of the 26th International Conference on the Physics of Semiconductors*, Institute of Physics Publishing, Bristol, UK and Philadelphia, PA. p. 61 (2002).
- ¹⁵N. R. Butler, P. Fisher, and A. K. Ramdas, *Phys. Rev. B* **12**, 3200 (1975).
- ¹⁶E. V. Demidov, M. C. Kuznetsov, V. V. Tsyplenkov, and V. N. Shastin, *Proceedings of the Workshop “Nanophysics”*, March 2006, IPM RAS, Nizhny Novgorod, Vol. 2, p. 320.
- ¹⁷T. O. Klaassen, J. N. Hovenier, S. G. Pavlov, E. E. Orlova, R. Kh. Zhukavin, A. V. Muravjov, V. N. Shastin, H.-W. Hübers, H. Riemann, and A. F. G. van der Meer, *Conference Digest of the 28th International Conference on Infrared and Millimeter Waves*, edited by N. Hiromoto, Otsu, Japan, JSAP Catalog No. 031231, 2003, p. 195.
- ¹⁸Z. C. Jagannath, W. Grabovski, and A. K. Ramdas, *Phys. Rev. B* **23**, 2082 (1981).
- ¹⁹A. J. Mayur, M. Dean Sciacca, A. K. Ramdas, and S. Rodriguez, *Phys. Rev. B* **48**, 10893 (1993).
- ²⁰E. M. Gershenson, A. P. Mel'nikov, and R. I. Rabinovich, in *Electron-Electron Interactions in Disordered Systems*, edited by A. L. Efros and M. Pollak (Elsevier Science, Amsterdam, 1985).
- ²¹R. Kh. Zhukavin, S. G. Pavlov, K. A. Kovalevsky, H.-W. Hübers, H. Riemann, and V. N. Shastin, *J. Appl. Phys.* **97**, 113708 (2005).